This article has been accepted for publication in a future issue of this journal, but has not been fully edited. Content may change prior to final publication. Citation information: DOI 10.1109/TPEL.2013.2286159, IEEE Transactions on Power Electronics

Virtual Flux Droop Method – A New Control Strategy of Inverters in Microgrids

Jiefeng Hu, Jianguo Zhu, *Senior Member, IEEE*, David G. Dorrell, *Senior Member, IEEE*, and Josep M. Guerrero, *Senior Member, IEEE*

***Abstract*—The parallel operation of inverters in microgrids is mainly based on the droop method. Conventional voltage droop method consists of adjusting the output voltage frequency and amplitude to achieve autonomous power sharing without control wire interconnections. Nevertheless, the conventional voltage droop method shows several drawbacks, such as complicated inner multiloop feedback control, and most importantly, frequency and voltage deviations. This paper proposes a new control strategy in microgrid applications by drooping the virtual flux instead of the inverter output voltage. First, the relationship between the inverter virtual flux and the active and reactive powers is mathematically obtained. This is used to develop a new flux droop method. In addition, a small-signal model is developed in order to design the main control parameters and study the system dynamics and stability. Furthermore, a direct flux control (DFC) algorithm is employed to regulate the virtual flux according to the droop controller, which avoids the use of PI controllers and PWM modulators. Both the simulation and experimental results shows that the proposed flux droop strategy can achieve active and reactive power sharing with much lower frequency deviation than the conventional voltage droop method, thus highlighting the potential use in microgrid applications.**

***Index Terms*—Microgrids, flux droop, active and reactive power sharing, power quality**

I. Introduction

A MICROGRID is a cluster of microgenerators connected to the local low voltage network through power electronic converters. Compared to a single distributed generation (DG) unit, microgrids offer many technical advantages in terms of control flexibility and the ability to incorporate renewable energy sources [1]-[3]. However, power quality and system stability have become serious issues due to the intermittent nature of the renewable energy sources and the fluctuating load profile. In addition, as the penetration and capacities of DG units increase, the power converters are required to operate more efficiently and effectively to maintain high power quality and dynamic stability. To fulfill these requirements, advanced control techniques are essential.

Several inverter control strategies are used in microgrids to achieve correct power sharing between the DG units. The majority of the strategies are derived from uninterruptible power supply (UPS) control schemes, such as circular chain control (3C) [4][5], average load sharing (ALS) [6][7], centralized [8], master-slave (MS) [9]-[11], and droop control [12]-[16]. Droop control is one of the most popular techniques in microgrid applications. This concept stems from power system theory, in which a synchronous generator connected to the utility grid drops its frequency when the power demand increases. The conventional droop method was first introduced into microgrids in [12], where active power sharing between the inverters is achieved by adjusting the frequency and reactive power sharing is achieved by adjusting the amplitude of the inverter output voltage. The droop method achieves relatively high reliability and flexibility since it uses only local power measurements.

However, the conventional droop method has several drawbacks, such as complicated inner multiloop feedback control, and most importantly, frequency and voltage deviations. To produce the specified voltage from the droop controller, a multiloop feedback control scheme is generally employed to control the inverters [13]-[17]. In the multiloop feedback control, proportional-integral (PI) regulators are used in the outer voltage loop and inner current loop. In addition, modulation such as sinusoidal pulse-width-modulation (SPWM) is required to generate the final gate drive signals. As a result, this method requires complex coordinate transformation, and much tuning effort is needed to ensure the system stability, which makes it difficult to implement in practice. Furthermore, it is well known that good power sharing is achieved when using the conventional droop method, but this does lead to degradation of the voltage regulation because the frequency and amplitude of the inverter output voltage are controlled directly. The voltage deviation could be unacceptable in applications where power quality is the main concern.

In recent years much research attention has been paid to the

J. Hu, J. Zhu, and D. G. Dorrell are with the Faculty of Engineering and Information Technology, University of Technology, Sydney, N.S.W., 2007, Australia. (e-mail: Jiefeng.Hu@uts.edu.au; Jianguo.Zhu@uts.edu.au; David.Dorrell@uts.edu.au).

J. M. Guerrero is with the Institute of Energy Technology, Aalborg University, 9220 Aalborg East, Denmark. (email: joz@et.aau.dk).

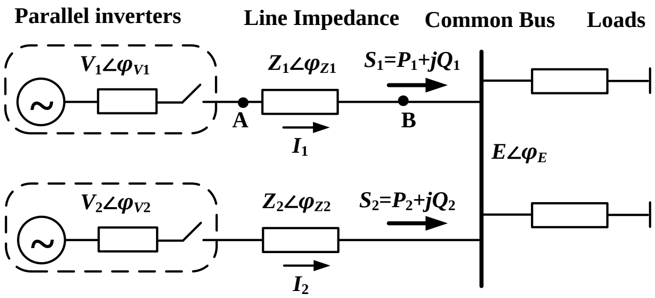

Fig. 1. Equivalent circuit of two parallel connected inverters in microgrids.

improvement the voltage droop method on order to obtain better dynamic response and steady-state performance. For example, better transient response was obtained by introducing the derivative-integral terms into the droop controller [18]-[20]. In order to increase the power sharing accuracy by decoupling the active and reactive powers, a virtual power frame transformation or virtual impedance method was introduced [21]-[24]. In [25], an angle controller was proposed to minimize frequency variation by drooping the inverter output voltage phase angle instead of the frequency. Consequently, the power quality was improved considerably. The main drawback is that other inverter initial phase angles are not known. To overcome this, a GPS signal can be used to obtain synchronization [25]. In [26]-[28], a multilayer control strategy was presented to compensate for the voltage deviation caused by the droop characteristics. Microgrid synchronization to a grid was introduced in [20] and [29]. All the methods mentioned above were developed using the voltage droop method, i.e., using $P-\omega$ and $Q-V$ characteristics. Therefore, complex multi-feedback loops are unavoidable; good power sharing is achieved at the expense of voltage deviation.

More recently a new virtual flux droop method was proposed [30]. This can achieve similar autonomous power sharing to conventional voltage droop control, but the frequency deviation is much lower. The control structure is very simple and without multi-feedback loops; hence, PI controllers are avoided and PWM modulators are also eliminated. Here, the theory is further developed and the new strategy is simulated, implemented and experimentally validated. This paper is organized as follows. In Section II, the relationship between the power flow and the inverter flux is derived, and this is used to develop a new virtual flux droop method. In Section III, the small signal model is developed to help calculate the control parameters and study system stability. In Section IV, a direct flux control scheme is presented. This controls the inverters in order to produce the required virtual flux from the droop controller. In Section V, the whole control strategy of the microgrid is illustrated by incorporating the proposed virtual flux droop method with the direct flux control scheme. In Section VI, the effectiveness of the proposed strategy is verified numerically by using MATLAB/Simulink and experimentally validated using a laboratory prototype.

II. Proposed Virtual Flux Droop Method

Fig. 1 shows two DG units connected to a common ac bus through their inverters. The mathematical equations of the system equivalent circuit can be described by

$$\boldsymbol{V} = R\boldsymbol{I} + L\frac{d\boldsymbol{I}}{dt} + \boldsymbol{E} \tag{1}$$

$$\boldsymbol{S} = P + jQ = \boldsymbol{I}^{*}\boldsymbol{E} \tag{2}$$

where $\boldsymbol{V}$, $\boldsymbol{E}$, and $\boldsymbol{I}$ are the inverter voltage vector, the common ac bus voltage vector, and the line current vector, respectively. Z is impedance of the transmission line where $Z = (R + j\omega L)$. P and Q are the active and reactive powers flowing from the DG to the common ac bus and * denotes the complex conjugate. In a similar manner to the flux definition in an electrical machine, the virtual flux vectors at nodes A and B can be defined as

$$\boldsymbol{\psi}_V = \int_{-\infty}^{t} \boldsymbol{V} d\tau \tag{3}$$

$$\boldsymbol{\psi}_E = \int_{-\infty}^{t} \boldsymbol{E} d\tau \tag{4}$$

From (3) and (4), the inverter virtual flux vector at node A and the common ac bus virtual flux vector at node B can be rewritten:

$$\varphi_{fV} = \varphi_V - \frac{\pi}{2}, \ |\boldsymbol{\psi}_V| = \frac{|\boldsymbol{V}|}{\omega} \tag{5}$$

$$\varphi_{fE} = \varphi_E - \frac{\pi}{2}, \ |\boldsymbol{\psi}_E| = \frac{|\boldsymbol{E}|}{\omega} \tag{6}$$

where φ_V and φ_E are the phase angles of $\boldsymbol{V}$ and $\boldsymbol{E}$; and φ_{fV} and φ_{fE} are the phase angles of $\boldsymbol{\psi}_V$ and $\boldsymbol{\psi}_E$, respectively. ω is the angular frequency of the voltages. In most practical cases, the line impedance is highly inductive, so the line resistance R can be neglected. Combining (1), (3) and (4) yields

$$\boldsymbol{I} = \frac{1}{L}(\boldsymbol{\psi}_V - \boldsymbol{\psi}_E) \tag{7}$$

Substituting (7) into (2), the volt-amps, or apparent power, can be obtained:

$$\boldsymbol{S} = \frac{1}{L}(\boldsymbol{\psi}_V - \boldsymbol{\psi}_E)^{*}\boldsymbol{E} \tag{8}$$

Subsequently, substituting (5) and (6) into (8) gives

$$\boldsymbol{S} = \frac{1}{L}\left(|\boldsymbol{\psi}_V| e^{j(\varphi_V - \frac{\pi}{2})} - |\boldsymbol{\psi}_E| e^{j(\varphi_E - \frac{\pi}{2})}\right)^{*} \omega |\boldsymbol{\psi}_E| e^{j\varphi_E} \tag{9}$$

This article has been accepted for publication in a future issue of this journal, but has not been fully edited. Content may change prior to final publication. Citation information: DOI 10.1109/TPEL.2013.2286159, IEEE Transactions on Power Electronics

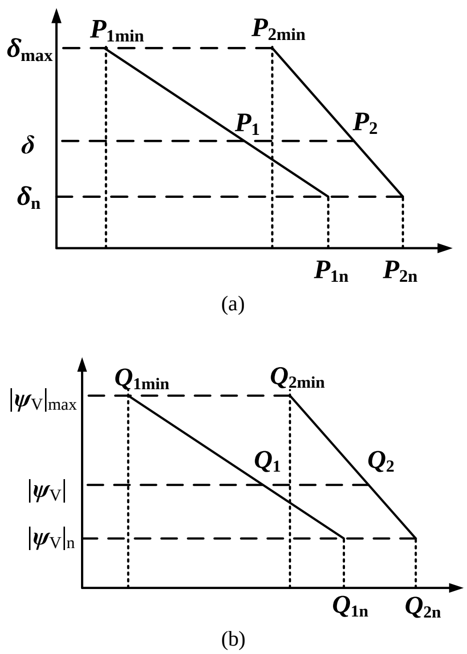

Fig. 2. Active and reactive power sharing with proposed flux droop method. (a) $P - \delta$ characteristic, (b) $Q - |\psi_V|$ characteristic.

so that

$$\boldsymbol{S} = \frac{\omega}{L}\left[|\psi_E||\psi_V|e^{j(\frac{\pi}{2}+\varphi_E-\varphi_V)} - |\psi_E|^2 e^{j(\frac{\pi}{2}+\varphi_E-\varphi_E)}\right] \tag{10}$$

Therefore, the apparent power flowing from the DG unit to the common ac bus can be derived from (10) giving

$$\boldsymbol{S} = \frac{\omega}{L}\left[|\psi_E||\psi_V|\sin(\varphi_V-\varphi_E) + j\left(|\psi_E||\psi_V|\cos(\varphi_V-\varphi_E) - |\psi_E|^2\right)\right] \tag{11}$$

The active power and reactive power can be obtained by decomposing (11) into real and imaginary components which leads to

$$P = \frac{\omega}{L}|\psi_E||\psi_V|\sin\delta \tag{12}$$

$$Q = \frac{\omega}{L}\left(|\psi_E||\psi_V|\cos\delta - |\psi_E|^2\right) \tag{13}$$

where $\delta = \varphi_V - \varphi_E = \varphi_{fV} - \varphi_{fE}$. Since this angular difference is typically small it can be assumed that $\sin(\delta) \approx \delta$ and $\cos(\delta) \approx 1$ so that

$$P = \frac{\omega}{L}|\psi_E||\psi_V|\delta \tag{14}$$

$$Q = \frac{\omega|\psi_E|}{L}\left(|\psi_V| - |\psi_E|\right) \tag{15}$$

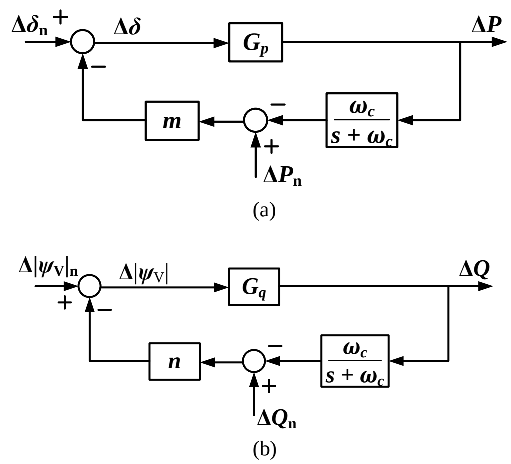

Fig. 3. Diagram illustration of small signal model, (a) $P - \delta$ droop controller, (b) $Q - |\psi_V|$ droop controller.

Therefore, the active power is proportional to the flux phase angle difference δ and the reactive power is proportional to the flux magnitude difference ($|\psi_V|$ - $|\psi_E|$). Based on the analysis above, a new droop method by drooping the inverter virtual flux is proposed here. This gives

$$\delta = \delta_n - m(P_n - P) \tag{14}$$

$$|\psi_V| = |\psi_V|_n - n(Q_n - Q) \tag{15}$$

where δ_n is the nominal phase angle difference between ψ_V and ψ_E, and $|\psi_V|_n$ is the nominal amplitude of the inverter flux. P_n and Q_n are the power rating of the DG unit; and m and n are the slopes of the $P - \delta$ and the $Q - |\psi_V|$ characteristics. The proposed flux droop method is illustrated in Fig. 2. The active power and reactive power are split between the DGs by drooping their own flux angle difference δ and flux amplitude $|\psi_V|$ when the load is changed.

III. Small Signal Analysis

A small signal analysis is now proposed in order to investigate the stability and transient response of the system. This allows the adjustment the control parameters. The small-signal dynamics of the $P - \delta$ droop controller can be obtained by linearizing (12) and (16). This gives

$$\Delta\delta(s) = \Delta\delta_n(s) - m(\Delta P_n(s) - \Delta P(s)) \tag{18}$$

$$\Delta P(s) = G_p \cdot \Delta\delta(s) \tag{19}$$

where $G_p = \frac{\omega}{L}|\psi_E||\psi_V|\cos\delta$. Modeling the low-pass filters as a first-order approximation for the instantaneous active power calculation, the $P - \delta$ droop controller equivalent circuit resulting from the small signal model is illustrated in Fig. 3(a), where Δ denotes the perturbation values, and ω_c is the cut-off angular frequency of the low-pass filters. By deriving the

This article has been accepted for publication in a future issue of this journal, but has not been fully edited. Content may change prior to final publication. Citation information: DOI 10.1109/TPEL.2013.2286159, IEEE Transactions on Power Electronics

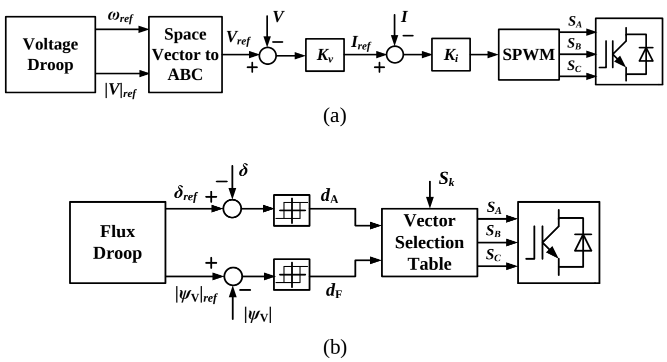

Fig. 4. Schematic diagram of control strategies of inverters, (a) multiloop feeback control for conventional voltage droop method, (b) direct flux control for proposed virtual flux droop method.

closed-loop transfer function using ΔP as the output and $\Delta\delta_n$ and ΔP_n as the inputs, using the principle of superposition, the following expression is obtained:

$$\Delta P(s) = \frac{G_p(s+\omega_c)}{s+\omega_c-\omega_c mG_p}\Delta\delta_n(s) - \frac{mG_p(s+\omega_c)}{s+\omega_c-\omega_c mG_p}\Delta P_n(s) \quad (20)$$

The characteristic equation can be derived from (20) where

$$s+\omega_c-\omega_c mG_p = 0 \quad (21)$$

Subsequently, the eigenvalue of (21) can be expressed as

$$\lambda_p = \omega_c(mG_p - 1) \quad (22)$$

Similarly, the small-signal dynamics of the $Q-|\psi_V|$ droop controller can be obtained by linearizing (13) and (17):

$$\Delta|\psi_V|(s) = \Delta|\psi_V|_n(s) - n(\Delta Q_n(s) - \Delta Q(s)) \quad (23)$$

$$\Delta Q(s) = G_q \cdot \Delta|\psi_V|(s) \quad (24)$$

where $G_q = \frac{\omega}{L}|\psi_E|\cos\delta$. Using a similar procedure, the $Q-|\psi_V|$ droop controller block diagram of the small signal model is illustrated in Fig. 3(b). Again, by deriving the closed loop transfer function using ΔQ as the output and $\Delta|\psi_V|_n$ and ΔQ_n as the input, and using the superposition principle, then

$$\Delta Q(s) = \frac{G_q(s+\omega_c)}{s+\omega_c-\omega_c nG_q}\Delta|\psi_V|_n(s) - \frac{nG_q(s+\omega_c)}{s+\omega_c-\omega_c nG_q}\Delta Q_n(s) \quad (25)$$

and characteristic equation can be derived:

$$s+\omega_c-\omega_c nG_q = 0 \quad (26)$$

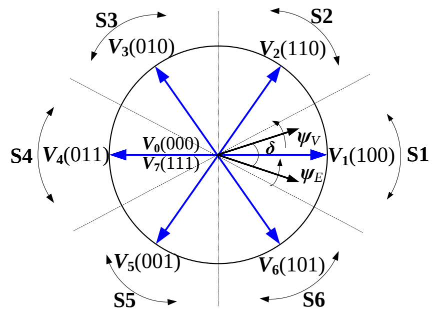

Fig. 5. Possible voltage vectors generated by the inverter and sectors division.

TABLE I. Vector Selection Strategy

Sector number (Location of $\boldsymbol{\psi}_V$)	S1	S2	S3	S4	S5	S6
d_F = 1 (Increase $\lvert\boldsymbol{\psi}_V\rvert$)	$\boldsymbol{V}_2$	$\boldsymbol{V}_3$	$\boldsymbol{V}_4$	$\boldsymbol{V}_5$	$\boldsymbol{V}_6$	$\boldsymbol{V}_1$
d_F = 0 (Decrease $\lvert\boldsymbol{\psi}_V\rvert$)	$\boldsymbol{V}_3$	$\boldsymbol{V}_4$	$\boldsymbol{V}_5$	$\boldsymbol{V}_6$	$\boldsymbol{V}_1$	$\boldsymbol{V}_2$
Zero vector is applied to when d_A = 0						

Hence, the eigenvalue of (26) is

$$\lambda_q = \omega_c(nG_q - 1) \quad (27)$$

It can be seen from (22) and (27) that the eigenvalue placements of system varies with the droop slopes m and n, illustrating the stability limits which can be used to adjust the transient response of the system.

IV. Direct Flux Control of Inverters

After obtaining the flux reference from the droop controller, the inverter is controlled to produce this flux in order to achieve the correct power sharing between the DG units. In the conventional voltage droop method, the frequency and the amplitude of the inverter output voltage are regulated for power sharing so that a multiloop feedback approach is used to control the inverters, as illustrated in Fig. 4(a). For the proposed virtual flux droop method, since the output of the droop controller is the flux reference rather than the voltage reference, a direct flux control (DFC) strategy can be employed to generate this specific flux, as depicted in Fig. 4(b).

For ease of illustration of the DFC approach, Fig. 5 shows three-phase two-level inverter voltage vectors and the spatial relationship of ψ_V and ψ_E. Using DFC, the two variables directly controlled by the inverter are $|\psi_V|$ and δ, i.e., the magnitude of vector ψ_V is controlled and it also has a specified relative position to the vector ψ_E. Similarly to direct torque control (DTC) [31] [32] and direct power control (DPC) [33] [34], the DFC strategy is based on the fact that the effects of each inverter voltage vector on $|\psi_V|$ and δ are different. This is summarized in Table I [12], where Sk is the sector number in the $\alpha-\beta$ plane given by φ_{fV}, being d_F =1 if $|\psi_V|_{ref} > |\psi_V|$, d_F=0 if $|\psi_V|_{ref} < |\psi_V|$; and d_A=1 if $\delta_{ref} > \delta$, d_A=0 if $\delta_{ref} < \delta$.

The DFC approach can be implemented in the following

This article has been accepted for publication in a future issue of this journal, but has not been fully edited. Content may change prior to final publication. Citation information: DOI 10.1109/TPEL.2013.2286159, IEEE Transactions on Power Electronics

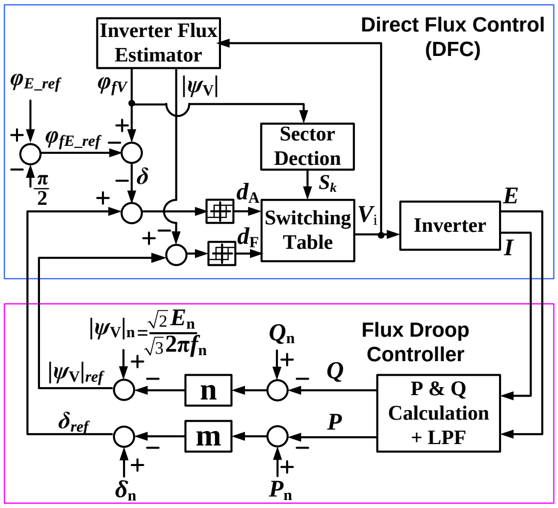

Fig. 6. Block diagram of the proposed microgrid control strategy.

way. The signals d_F and d_A are first obtained from two hysteresis comparators using the errors between the estimated and reference values of $|\psi_V|$ and δ. The voltage vector is then selected from Table I according to d_F, d_A and the inverter flux position φ_{fV}. For instance, assuming that at the k^{th} sampling instant, φ_{fV} is within sector S1, $|\psi_V|_{ref} > |\psi_V|$ and $\delta_{ref} > \delta$, so that d_F =1 and d_A=1. Therefore $\boldsymbol{V}_2$(110) will be selected to increase both $|\psi_V|$ and δ. After that $\boldsymbol{V}_2$(110) will be applied during the k^{th} and $(k+1)^{th}$ sampling instants. In a similar manner DTC and DPC, this voltage vector can be generated simply by turning on the upper switches and turning off the lower switches of the inverter legs of phases *A* and *B*, while turning off the upper switch and turning on the lower switch of phase *C*. In this way, $\boldsymbol{\psi}_V$ is controlled around an approximate circular path within specified hysteresis bands through the inverter switching DFC features excellent dynamic performance without coordinate transformations or PWM modulators.

V. Microgrid Control

Fig. 6 shows a block diagram of the proposed control strategy for microgrid connection, it includes the virtual flux droop method presented in Section II and the DFC scheme presented in Section IV. In the virtual flux droop controller, the active and reactive powers *P* and *Q* supplied by the DGs to the load are calculated from the line current $\boldsymbol{I}$ and load-side voltage $\boldsymbol{E}$, and then delivered to the flux droop function to obtain the flux reference. In the DFC strategy, the flux is firstly estimated from the current inverter switching states [35], this estimated flux together with the flux reference from the droop controller are then sent to the DFC controller to control the inverter.

Notice that there is a no load-side ac voltage available to reference. The inverters themselves produce the ac system voltage. By using the proposed control strategy, the load-side ac voltage $\boldsymbol{E}$ is controlled indirectly because $\boldsymbol{\psi}_E$ is already regulated due to the direct control of $\boldsymbol{\psi}_V$.

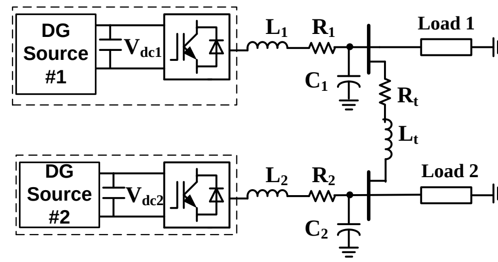

Fig. 7. Microgrid structure under study.

TABLE II
System Parameters

Item	Symbol	Simulation	Experiment
Line inductance	L_1, L_2	8 mH	5 mH
Line resistance	R_1, R_2	0.05Ω	0.48 Ω
Filter Capacitance	C_1, C_2	150 μF	82 μF
Tie-line inductance	L_t	6 mH	5.5 mH
Tie-line resistance	R_t	0.4Ω	0.36 Ω
Nominal Voltage	E_n	3.6 kVrms	120 Vrms
Nominal frequency	f_n	60 Hz	60 Hz
DGs output voltage	V_{dc1}, V_{dc2}	10 kV	250 V
Cut-off frequency	ω_c	10 rad/s	10 rad/s
Nominal flux amplitude	$\|\psi_V\|_n$	7.797 Wb	0.312 Wb
Nominal angle difference	δ_n	0.2 rads	0.2 rads
Nominal active power	P_{1n}	1.5 MW	180 W
Nominal reactive power	Q_{1n}	0.8 MVAr	100 VAr
Nominal active power	P_{2n}	1.2 MW	150 W
Nominal reactive power	Q_{2n}	0.6 MVAr	70 VAr
Slope of $P-\delta$ droop	m_1	-2.67×10^{-7} rad/W	-2.2×10^{-3} rad/W
Slope of $Q-\|\psi_V\|$ droop	n_1	-2.65×10^{-7} Wb/VAr	-1.52×10^{-4} Wb/VAr
Slope of $P-\delta$ droop	m_2	-3.33×10^{-7} rad/W	-3.1×10^{-3} rad/W
Slope of $Q-\|\psi_V\|$ droop	n_2	-9.55×10^{-7} Wb/VAr	-1.76×10^{-4} Wb/VAr

i) Amplitude Regulation: the amplitude of the load-side voltage $\boldsymbol{E}$ can be controlled by setting the nominal inverter flux amplitude $|\psi_V|_n$ equal to $\sqrt{2}E_n/(\sqrt{3}\cdot 2\pi f_n)$, where E_n is the nominal line-to-line voltage of the microgrid.

ii) Frequency Regulation: the referenced φ_{fE_ref} is taken from a referenced virtual three-phase ac voltage with f_n = 60 Hz. It can be calculated from $\varphi_{fE\_ref} = \varphi_{E\_ref} - \pi/2$ using (6). In this way, $\boldsymbol{\psi}_E$ can be controlled with a specific frequency f_n because δ is tightly regulated, thus the frequency of the load-side voltage $\boldsymbol{E}$ can be controlled.

An in-depth analysis of the proposed flux droop method (16) in Section II can now be performed. It can be seen that, in contrast to the conventional voltage droop method, the active power sharing of the microgrid is achieved by drooping the angle difference δ rather than drooping the frequency. Since the reference φ_{fE_ref} is taken from a virtual reference three-phase ac voltage vector with a constant frequency f_n, both the vector $\boldsymbol{\psi}_V$ and vector $\boldsymbol{\psi}_E$ will rotating with a constant

This article has been accepted for publication in a future issue of this journal, but has not been fully edited. Content may change prior to final publication. Citation information: DOI 10.1109/TPEL.2013.2286159, IEEE Transactions on Power Electronics

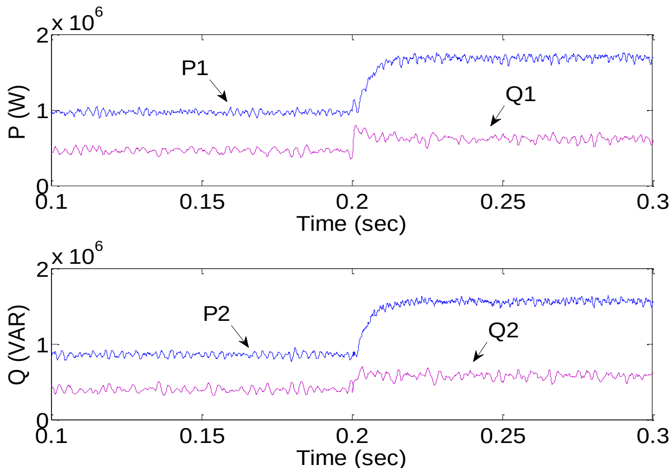

Fig. 8. Simulated dynamic response of the active and reactive powers supplied by DGs for load step changes.

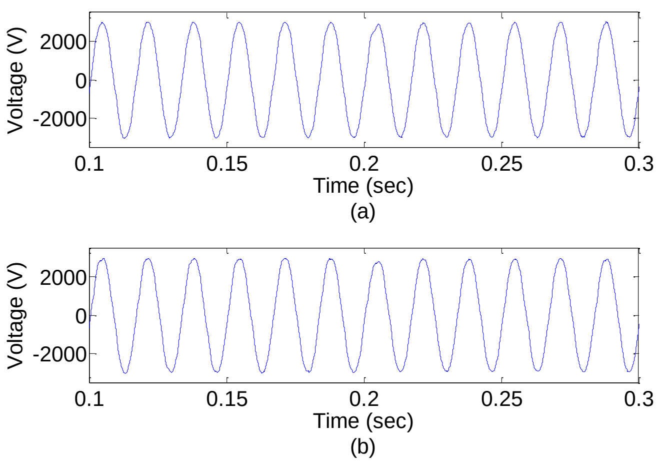

Fig. 9. Performance of the load-side voltages, i.e., the voltages across the capacitors, (a) phase A voltage of C1, (b) phase A voltage of C2

angular frequency because δ is tightly controlled. In other words, the angular frequency ψ_E will not be changed no matter how δ has changed. Consequently, active power sharing can be achieved without frequency deviation, even though the initial flux phase of each inverter is unknown. This is a significant improvement in microgrid power control.

VI. Simulation Results

Fig. 7 shows the microgrid structure under study, which is the same as that in [12]. The performance of the proposed flux droop control strategy was first tested in simulation using MATLAB/Simulink. The system parameters are listed in Table II. The system sampling frequency is 20 kHz and the average switching frequency of each inverter is about 3.2 kHz.

Fig. 8 shows the powers sharing between two inverters for a load step change at 0.2 s. It is found that the two DGs can take up the load change immediately, and the system reaches a new steady-state point within only 10 ms. DG #1 delivers more

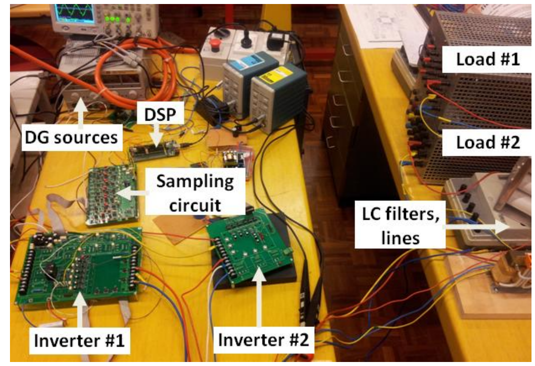

Fig. 10. Laboratory microgrid setup.

active power because it has a steeper slope, as explained in Section II. This result demonstrates the effectiveness of the novel flux droop method for autonomous power sharing in microgrid applications. Fig. 9 shows the performance of the load-side voltage (i.e., the voltage across the dc link capacitors). It can be seen that the voltage established is very stable and sinusoidal before, during and after the load changes. This benefits the local microgrid customers.

VII. Experimental Results

The proposed control strategy is further validated experimentally on a scaled laboratory prototype, as shown in Fig. 10. A TMS320F28335 floating-point DSP was used for the control. This includes six enhanced PWM modules (each ePWM module contains two reversed PWM channels) and sixteen analog-to-digital (AD) channels, which are sufficient for the gate drives and measurement in this test. The system parameters are listed in Table II.

A. *Transient Response of Power Sharing*

Autonomous power sharing is the most important feature in the smart microgrid systems. In other words, the changes in load should be taken up by the distributed generation (DG) units automatically [12], [18]. Here, the effectiveness of the proposed virtual flux droop method for autonomous power sharing is tested. Fig. 11 presents the dynamic response of the power sharing when a step-up change of the load occurs. P_1 and Q_1 are the active and reactive power outputs of DG1, while P_2 and Q_2 are active and reactive power outputs of DG2. It can be seen that the experimental results are in good agreement with the simulation results. To meet the new load demand, DG1 and DG2 pick up the load change immediately with excellent dynamic response and steady-state performance.

In order to further prove the effectiveness of the proposed control strategy, the load demand was reduced to the initial value. As shown in Fig. 12, the outputs of the DG1 and DG2 are reduced accordingly and the system reaches the new steady-state very quickly and smoothly without any overshoot.

B. *Steady State Performance*

To analyze the voltage quality, the line-to-line voltage across

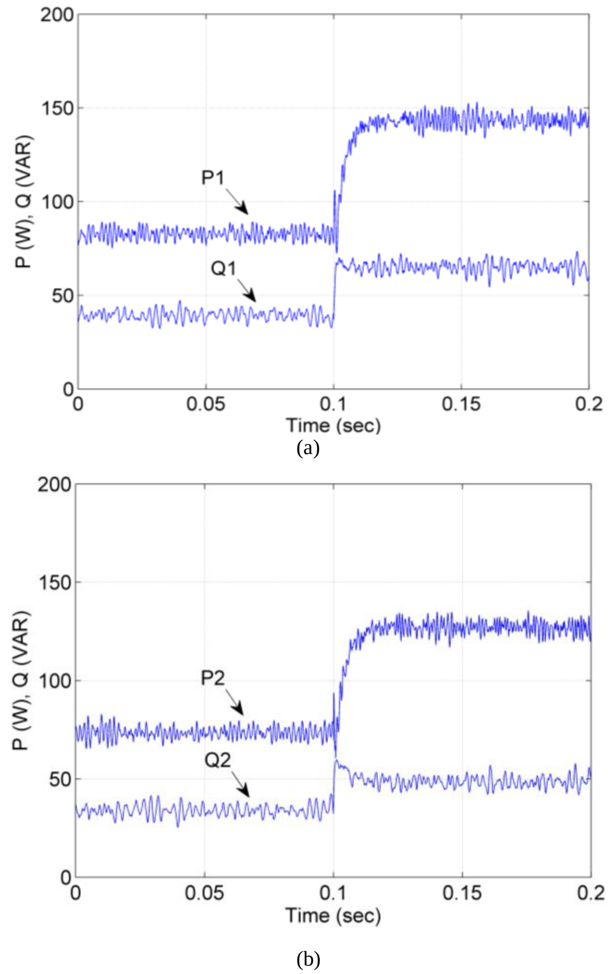

Fig. 11. Experimental dynamic response when the load demand increased, (a) DG1 output powers, (b) DG2 output powers.

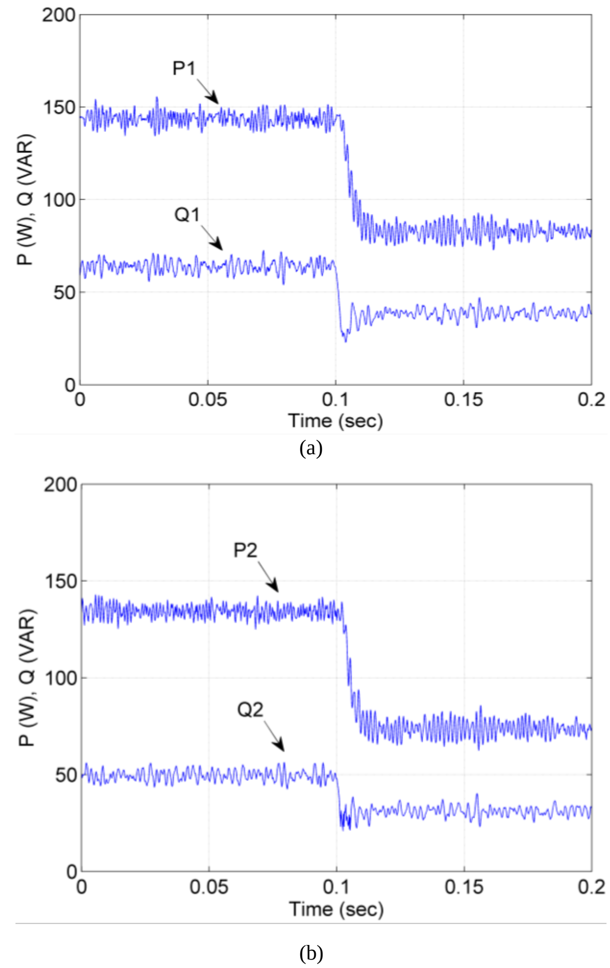

Fig. 12. Experimental dynamic response when the load demand decreased, (a) DG1 output powers, (b) DG2 output powers.

the capacitor C_1 of DG1 (i.e., the voltage of load #1) is plotted out and shown in Fig. 13(a). It can be observed that the voltage established for load #1 is very stable and sinusoidal with only 1.83% of the total harmonic distortion (THD). Fig. 13(b) is the spectrum of the voltage waveforms. It shows broad harmonic spectra due to the varied switching frequencies of DFC scheme, as depicted in Section IV. The voltage of load #2 is similar to that of load #1, which is not plotted out here.

C. Voltage Quality Comparison

In order to show that the proposed virtual flux droop control strategy can achieve better power quality for autonomous power sharing in microgrids, Table III compares the voltage frequency and amplitude deviations by using the conventional voltage droop method and the proposed flux droop method, respectively. For this purpose, a load variation on a step change will be demanded, and the voltage responding to that load change in order to achieve autonomous power sharing will be compared. In the first case, it can be seen that there is around 2.5 V of voltage amplitude deviation in order to compensate 50 Var reactive power unbalance when the load is changed, for both the conventional $V-Q$ droop and the proposed $|\boldsymbol{\psi}_V| - Q$ droop. In the second case, in order to compensate 50 W active power unbalance when the load is changed, there is 0.40 Hz deviation of the frequency using conventional voltage droop method, while there is only 0.09 Hz deviation of the frequency using proposed flux droop method, showing much better voltage quality in terms of frequency stability. This is because in the proposed flux droop method, active power is regulated by drooping the phase angle of the virtual flux rather than the voltage frequency, as explained in Section V.

VIII. Conclusion

In this paper, a new flux droop control strategy for the parallel operation of inverters has been proposed for microgrid applications. This is different to the conventional voltage droop method. In the new flux droop controller, the power sharing is achieved by drooping the flux amplitude and controlling the phase angle. In addition, a direct flux control algorithm is introduced to control the inverters in order to produce a specified flux from droop controller. Therefore, multi-feedback loops and PWM modulators are not needed in the control structure. The new droop control strategy is simple and

This article has been accepted for publication in a future issue of this journal, but has not been fully edited. Content may change prior to final publication. Citation information: DOI 10.1109/TPEL.2013.2286159, IEEE Transactions on Power Electronics

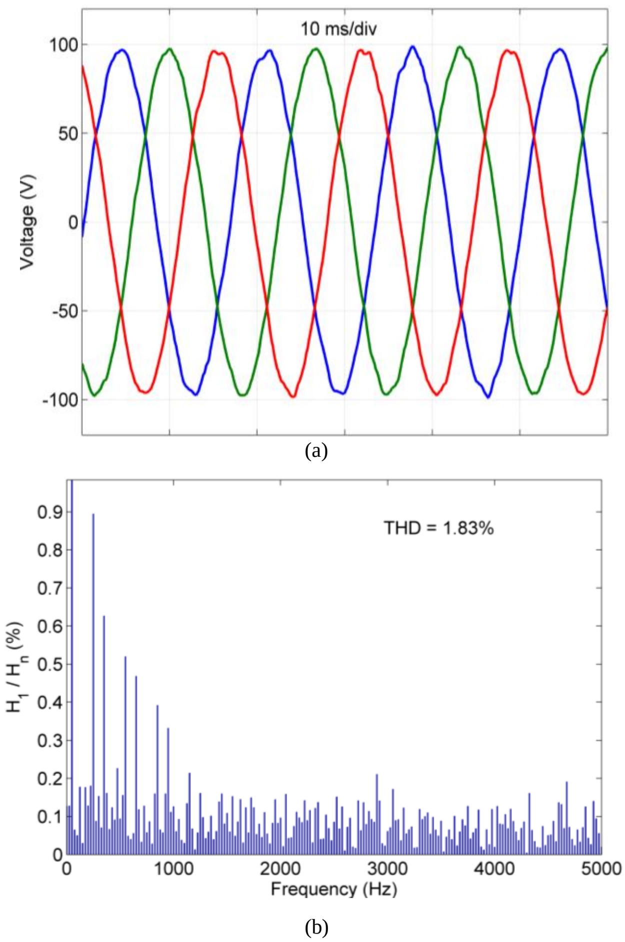

Fig. 13. Performance of the voltages of capacitor C_1 (i.e., voltage for load #1), (a) voltage waveforms, (b) spectrum, THD = 1.83%.

effective, the effectiveness is validated by using both simulation and experiments, highlighting the potential use in microgrid applications.

TABLE III

COMPARISON OF VOLTAGE DEVIATIONS WITH $\Delta P = 50$ W AND $\Delta Q = 50$ VAR

Methods	Frequency Deviations (Hz)	Amplitude Deviations (V)
Conventional Voltage droop	0.40	2.61
Proposed Virtual Flux droop	0.09	2.43

REFERENCES

[1] R. Lasseter, “Microgrids,” in *Proc. IEEE Power Eng. Soc. Winter Meet.*, 2002, pp. 305-308.

[2] N. Pogaku, M. Prodanovic, and T. C. Green, “Modeling, analysis and testing of autonomous operation of an inverter-based microgrid,” *IEEE Trans. Power Electron.*, vol. 22, no. 2, pp. 613-625, Mar. 2007.

[3] J. M. Guerrero, F. Blaabjerg, T. Zhelev, K. Hemmes, E. Monmasson, S. Jemei, M. P. Comech, R. Granadino, and J. I. Frau, “Distributed generation: Toward a new energy paradigm” *IEEE Mag. Ind. Electron.*, Vol. 4, No. 1, pp. 52-64, 2010.

[4] T. F. Wu, Y.-K. Chen, and Y.-H Huang, “3C strategy for inverters in parallel operation achieving an equal current distribution,” *IEEE Trans. Ind. Electron.*, vol. 47, no. 2, pp. 273-281, Apr. 2000.

[5] S. J. Chiang, C. H. Lin, and C. Y. Yen, “Current limitation control technique for parallel operation of UPS inverters,” in *Proc. IEEE PESC*, 2004, pp. 1922-1926.

[6] X. Sun, Y-S. Lee, and D. Xu, “Modeling, analysis, and implementation of parallel multi-inverter system with instantaneous average-current-sharing scheme,” *IEEE Trans. Power Electron.*, vol. 18, no. 3, pp. 844-856, May 2003.

[7] Z. He, Y. Xing, and Y. Hu, “Low cost compound current sharing control for inverters in parallel operation,” in *Proc. IEEE PESC*, 2004, pp. 222-227.

[8] T. Iwade, S. Komiyama, and Y. Tanimura, “A novel small-scale UPS using a parallel redundant operation system,” in *Proc. IEEE IEICE/IEEE INTELEC*, 2003, pp. 480-483.

[9] J. Holtz, W. Lotzkat, and K. H. Werner, “A high-power multitransistor-inverter uninterruptible power supply system,” *IEEE Trans. Power Electron.*, vol. 3, no. 3, pp. 278-285, Jul. 1988.

[10] S. Tamai and M. Kinoshita, “Parallel operation of digital controlled UPS system,” in *Proc. IEEE IECON*, 1991, pp. 326-331.

[11] Y. Pei, G. Jiang, X. Yang, and Z. Wang, “Auto-master-slave control technique of parallel inverters in distributed AC power systems and UPS,” in *Proc. IEEE PESC*, 2004, pp. 2050-2053.

[12] M. C. Chandorkar, D. M. Divan, and R. Adapa, “Control of parallel connected inverters in standalone ac supply systems,” *IEEE Trans. Ind. Appl.*, vol. 29, no. 1, pp. 136-143, Jan./Feb. 1993.

[13] A. Tuladhar, H. Jun, T. Unger, and K. Mauch, “Parallel operation of single phase inverter modules with no control interconnections,” in *Proc. IEEE APEC*, 1997, pp. 94-100.

[14] U. Borup, F. Blaabjerg, and P. N. Enjeti, “Sharing of nonlinear load in parallel-connected three-phase converters,” *IEEE Trans. Ind. Appl.*, vol. 37, no. 6, pp. 1817-1823, Nov./Dec. 2001.

[15] L. Mihalache, “Parallel control technique with no intercommunication signals for resonant controller-based inverters,” in *Conf. Rec. IEEE IPEMC*, 2004, pp. 956-959.

[16] J. Hu, J. Zhu, and G. Platt, “A droop control strategy of parallel-inverter-based micorgrid”, *Proc. of IEEE Int. Applied Superconductivity and Electromagnetic Devices (ASEMD) Conf.*, Sydney, Australia, pp. 188–191, 2011.

[17] C. N. Rowe, T. J. Summers, R. E. Betz, D. J. Cornforth, and T. G. Moore, “Arctan power-frequency droop for improved microgrid stability,” *IEEE Trans. Power Electron.*, vol. 28, no. 8, pp. 3747-3759, Aug. 2013.

[18] J. M. Guerrero, L. G. Vicuna, J. Matas, M. Castilla, and J. Miret, “A wireless controller to enhance dynamic performance of parallel inverters in distributed generation systems,” *IEEE Trans. Power Electron.*, vol. 19, no. 5, pp. 1205-1213, 2004.

[19] A. M. Salamah, S. J. Finney, and B. W. Williams, “Autonomous controller for improved dynamic performance of AC grid, parallel-connected, single-phase inverters,” *IET Gener. Trnasm. Distrib.*, vol. 2, no. 2, pp. 209-218, 2008.

[20] J. C. Vásquez, J. M. Guerrero, A. Luna, P. Rodríguez, and R. Teodorescu, “Adaptive droop control applied to voltage-source inverter operating in grid-connected and islanded modes” *IEEE Trans. Ind. Electron.*, vol. 56, no. 10, pp. 4088-4096, 2009.

[21] K. D. Brabandere, B. Bolsens, J. V. Keybus, A. Woyte, J. Driesen, and R. Belmans, “A voltage and frequency droop control method for parallel inverters,” *IEEE Trans. Power Electron.*, vol. 22, no. 4, pp. 1107-1115, 2007.

[22] Y. Li and C. N. Kao, “An accurate power control strategy for power-electronics-interfaced distributed generation units operating in a low-voltage multibus microgrid,” *IEEE Trans. Power Electron.*, vol. 24, no. 12, pp. 2977-2988, 2009.

[23] J. M. Guerrero, L. Hang, and J. Uceda, “Control strategy for flexible microgrid based on parallel line-interactive UPS systems,” *IEEE Trans. Ind. Electron.*, vol. 56, no. 3, pp. 726-736, March 2009.

[24] J. He and Y. W. Li, “An enhanced microgrid load demand sharing strategy,” *IEEE Trans. Power Electron.*, vol. 27, no. 9, pp. 3984-3995, Sept. 2012.

[25] R. Majumder, B. Chaudhuri, A. Ghosh, R. Majumder, G. Ledwich, and F. Zare, “Improvement of stability and load sharing in an autonomous microgrid using supplementary droop control loop,” *IEEE Trans. Power System.*, vol. 25, no. 2, pp. 796-808, 2010.

[26] M. Savaghebi, A. Jalilian, J. C. Vasquez, and J. M. Guerrero, “Secondary control for voltage quality enhancement in microgrids,” *IEEE Trans. Smart Grid.*, vol. 3, no. 4, pp. 1893-1902, Dec. 2012.

[27] M. Hua, H. Hu, Y. Xing, and J. M. Guerrero, “Multilayer control for inverters in parallel operation without intercommunications,” *IEEE Trans. Power Electron.*, vol. 27, no. 8, pp. 3651-3663, August 2012.

This article has been accepted for publication in a future issue of this journal, but has not been fully edited. Content may change prior to final publication. Citation information: DOI 10.1109/TPEL.2013.2286159, IEEE Transactions on Power Electronics

[28] Q. Shafiee, J. M. Guerrero, and J. C. Vasquez, "Distributed secondary control for islanded microgrids – A novel approach," *IEEE Trans. Power Electron.,* vol. 29, no. 2, pp. 1018-1031, Feb. 2014.

[29] C. Cho, J.-H. Jeon, J.-Y. Kim, S. Kwon, K. Park, and S. Kim, "Active synchronizing control of a microgrid," *IEEE Trans. Power Electron.,* vol. 26, no. 12, pp. 3707-3719, Dec. 2011.

[30] J. Hu, J. Zhu, Y. Qu, and J. M. Guerrero, "A new virtual-flux-vector based droop control strategy for parallel connected inverters in microgrids," in *Proc. IEEE Energy Conversion Congress and Exposition (ECCE) Asia DownUnder.,* 2013, pp. 585-590.

[31] G. S. Buja and M. P. Kazmierkowski, "Direct torque control of PWM inverter-fed AC motors ─ A Survey," *IEEE Trans. Ind. Electron.,* vol. 51, no. 4, pp. 744-757, 2004.

[32] J. Hu, J. Zhu, Y. Zhang, G. Platt, Q. Ma and D. G. Dorrell, "Predictive direct virtual torque and power control of doubly fed induction generators for fast and smooth grid synchronization and flexible power regulation," *IEEE Trans. Power Electron.,* vol. 28, no. 7, pp. 3182–3194, July 2013.

[33] E. Tremblay, S. Atayde, and A. Chandra, "Comparative study of control strategies for the doubly fed induction generator in wind energy conversion systems: a DSP-based implementation approach," *IEEE Trans. Sustain. Energy,* vol. 2, no. 3, pp. 288-299, Jul. 2011.

[34] J. Hu, J. Zhu, G. Lei, G. Platt and D. G. Dorrell, "Multi-objective model-predictive control for high power converters," *IEEE Trans. on Energy Convers.,* vol. 28, no. 3, pp. 652-663, Sep. 2013.

[35] M. P. Kazmierkowski, R. Krishnan, and F. Blaabjerg, *Control in Power Electronics*. New York: Academic, 2002.

Jiefeng Hu (S'12) received the B.E. and M.E. degrees from Beijing University of Aeronautics & Astronautics, China, in 2007 and 2009, respectively, and the Ph.D. degree from University of Technology, Sydney (UTS), Australia, in 2013, all in electrical engineering.

In Oct. 2010, he was conferred the NSW/ACT Postgraduate Student Energy Awards by Australian Institute of Energy. From Jan. 2011 to Mar. 2013, he was involved in the research of the minigrid within Commonwealth Scientific and Industrial Research Organisation (CSIRO)'s Energy Transformed Flagship, Australia. Currently he is a Research Associate in UTS. His research interests include electric drives, control of power converters, and microgrids.

Jianguo Zhu (S'93-M'96-SM'03) received his BE in 1982 from Jiangsu Institute of Technology, China, ME in 1987 from Shanghai University of Technology, China, and Ph.D in 1995 from University of Technology, Sydney, Australia, all in electrical engineering.

He currently holds the positions of Professor of Electrical Engineering and Head for School of Electrical, Mechanical and Mechatronic Systems at UTS, Australia. His research interests include electromagnetics, magnetic properties of materials, electrical machines and drives, power electronics, and green energy systems.

David G. Dorrell (M'95-SM'08) received the B.E. (Hons.) degree from the University of Leeds, U.K., in 1988, the M. Sc. Degree from the University of Bradford, Bradford, U.K., in 1989, and the Ph.D. degree from The University of Cambridge, U. K., in 1993.

He has held lecturing positions with The Robert Gordon University and The University of Reading. He was a Senior Lecturer with The University of Glasgow, UK, for several years. In 2008 he took up a post with The University of Technology Sydney, Australia, and he was promoted to Associate Professor in 2009. His research interests cover the design and analysis of various electrical machines and also renewable energy systems with over 150 technical publications to his name. He is a Chartered Engineer in the UK and a Fellow of the Institution of Engineering and Technology.

Josep M. Guerrero (S'01–M'03–SM'08) was born in Barcelona, Spain, in 1973. He received the B.S. degree in telecommunications engineering, the M.S. degree in electronics engineering, and the Ph.D. degree in power electronics from the Technical University of Catalonia, Barcelona, in 1997, 2000 and 2003, respectively.

He was an Associate Professor with the Department of Automatic Control Systems and Computer Engineering, Technical University of Catalonia, teaching courses on digital signal processing, field-programmable gate arrays, microprocessors, and control of renewable energy. In 2004, he was responsible for the Renewable Energy Laboratory, Escola Industrial de Barcelona. He was a Visiting Professor with Zhejiang University, China, and the University of Cergy-Pontoise, France. Since 2011, he has been a Full Professor with the Department ofEnergy Technology, Aalborg University, Aalborg East, Denmark, where he is responsible for the microgrid research program. His research interests is oriented to different microgrid aspects, including power electronics, distributed energy- storage systems, hierarchical and cooperative control, energy management systems, and optimization of microgrids and islanded minigrids. Dr. Guerrero is an Associate Editor for the IEEE TRANSACTIONS ON POWER ELECTRONICS, the IEEE TRANSACTIONS ON INDUSTRIAL ELECTRONICS, and the IEEE Industrial Electronics Magazine. He has been Guest Editor of the IEEE TRANSACTIONS ON POWER ELECTRONICS Special Issues: Power Electronics for Wind Energy Conversion and Power Electronics for Microgrids, and the IEEE TRANSACTIONS ON INDUSTRIAL ELECTRONICS Special Sections: Uninterruptible Power Supplies systems, Renewable Energy Systems, Distributed Generation and Microgrids, and Industrial Applications and Implementation Issues of the Kalman Filter. He currently chairs the Renewable Energy Systems Technical Committee of the IEEE Industrial Electronics Society.